

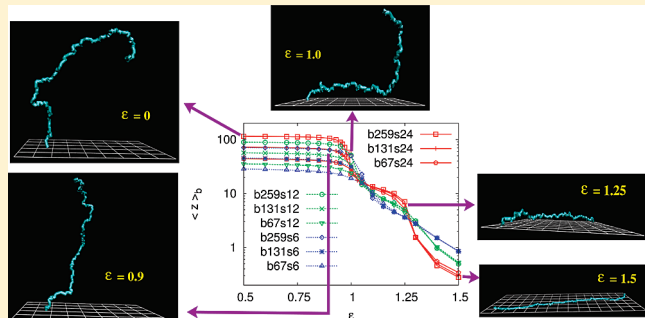
# Structure of Bottle Brush Polymers on Surfaces: Weak versus Strong Adsorption

Hsiao-Ping Hsu,<sup>\*,†</sup> Wolfgang Paul,<sup>‡</sup> and Kurt Binder<sup>†</sup>

<sup>†</sup>Institut für Physik, Johannes Gutenberg-Universität Mainz, 55099 Mainz, Staudinger Weg 7, Germany

<sup>‡</sup>Theoretische Physik, Martin Luther-Universität Halle-Wittenberg, von Seckendorff Platz 1, 06120 Halle, Germany

**ABSTRACT:** Large-scale Monte Carlo simulations are presented for a coarse-grained model of cylindrical molecular brushes adsorbed on a flat structureless substrate, varying both the chain length  $N$  of the side chains and the backbone chain length  $N_b$ . For the case of good solvent conditions, both the cases of weak adsorption (only 10 to 15% of the monomers being bound to the surface) and strong adsorption ( $\sim 40\%$  of the monomers being bound to the surface, forcing the bottle brush into an almost 2D conformation) are studied. We focus on the scaling of the total linear dimensions of the cylindrical brush with both chain lengths  $N$  and  $N_b$ , demonstrating a crossover from rod-like behavior (for not very large  $N_b$ ) to the scaling of 2D self-avoiding walks. Despite the fact that snapshot pictures suggest a “worm-like” picture as a coarse-grained description of such cylindrical brushes, the Kratky–Porod worm-like chain model fails because there is no regime where Gaussian statistics applies. We compare the stiffness (orientational correlations of backbone bonds, persistence length estimates, etc.) of the adsorbed bottle brush polymers with their corresponding 3D nonadsorbed counterparts. Consequences for the discussion of pertinent experiments are briefly discussed.



## 1. INTRODUCTION

Cylindrical brush molecules, the so-called “bottle brushes”, are macromolecules with a comblike architecture, where (flexible or stiff) side chains are densely grafted onto a long flexible main chain, the so-called “backbone”. (See refs 1–5 for recent reviews and more extensive documentation of literature.) There is a great freedom in the choice of the chemical species for the main chain and the side chains, and varying their molecular weights can vary both the overall size and the stiffness of these cylindrical brushes. There is a delicate interplay between configurational entropy, repulsive interactions (excluded volume), and attractive forces (mediated by the solvent). Therefore, the structure of these cylindrical brushes is very sensitive to solvent quality and other external stimuli, leading to various interesting possible applications.<sup>1,3,6,7</sup> We note that macromolecules with bottle brush architecture occur also in various biological contexts<sup>8–10</sup> and are believed to have important functions there.

It is of particular interest to consider molecular brushes adsorbed on substrates.<sup>11–18</sup> First of all, under many circumstances nanotechnological applications require that these molecules are attached to a flat solid surface, and biological functions often require that a biomolecule with this architecture is adsorbed at a cell membrane. Furthermore, for a surface-adsorbed conformation, additional experimental methods become available to directly visualize the (coarse-grained) molecular structure of these cylindrical brushes, such as scanning force microscopy<sup>3,11–16</sup> or measuring force versus extension curves

via atomic force tips linked to a backbone chain end.<sup>14</sup> Fascinating structures have been observed, such as a dense coiling into spirals<sup>11</sup> and spontaneously bent “meander-like” structures for which asymmetries between the numbers of side chains on both sides of the adsorbed backbone have been suggested<sup>17</sup> as a possible cause. Also, theoretical concepts for understanding the stiffness of adsorbed bottle brushes have been developed.<sup>18</sup> Although atomic force micrograph images of the ensemble of adsorbed bottle brushes, as amply presented in the literature (e.g., refs 3 and 11–16), give full information on their statistics on the coarse-grained scale, the interpretation is nevertheless subtle: the actual forces acting from the substrate on the monomers of the backbone and the (mostly chemically different) side chains are not explicitly known, and it is also not known whether the bottle brush polymer is “strongly adsorbed”, in the sense that the side chains assume essentially quasi-2D conformations or “weakly adsorbed” in the sense that the local cross-sectional monomer density profile resembles a section through a hemicylinder or sphere-cap shape, where most of the side chain monomers still occupy a 3D volume with a significant extension in the  $z$  direction perpendicular to the substrate. Another

**Special Issue:** H. Eugene Stanley Festschrift

**Received:** April 29, 2011

**Revised:** June 20, 2011

**Published:** July 13, 2011

problem is that the solvent conditions (good solvent versus  $\theta$  solvent versus poor solvent) are not always clear for bottle brushes adsorbed to substrates, remembering also the different chemical nature of backbone and side chains. Theta conditions in bulk 3D solution need not coincide with  $\theta$  conditions of a strongly adsorbed polymer. Also, the applicability of very simplified theoretical models, which completely neglect excluded volume effects, such as the Kratky–Porod<sup>19</sup> model of semiflexible chains that is widely used (e.g., ref 14), is questionable.<sup>5,20,21</sup>

Therefore, it would be useful to have more detailed theoretical studies:<sup>22–24</sup> monomer–substrate interactions can be precisely chosen, with respect to both their range and their strength, the solvent conditions can be precisely controlled as well, and the structure of the molecular brush is also accessible on the scale of individual monomers not only its large-scale coarse-grained properties. First simulation studies<sup>23,24</sup> indicated a scaling  $\langle R_{ee}^2 \rangle \propto N_b^{2\nu}$  for the end-to-end distance of the backbone of the adsorbed bottle brush where the (effective) exponent  $\nu$  is close to the value  $\nu_2 = 3/4$  expected for 2D self-avoiding walks.<sup>25</sup> Therefore, these (preliminary) studies did not give evidence of the suggestion<sup>16</sup> that the spontaneous curvature predicted for 2D molecular brushes<sup>13,17</sup> causes an exponent  $\nu \approx 0.53$ . However, Elli et al.<sup>23</sup> did consider only a single, very short, side chain length ( $N = 5$ ), and Hsu et al.<sup>24</sup> using  $N = 6$  to 48 considered primarily the configurational changes near the adsorption transition, and a systematic variation of the backbone chain length was not yet performed.

de Jong et al.<sup>26</sup> carried out a very pioneering study of a strictly 2D model of bottle brushes with flexible backbones but did consider a few selected choices of  $N_b$  and  $N$  only. For the case  $N_b = 100, N = 10$ , they compared a system, where the number of side chains at the left and right side of the backbone were strictly equal and fixed to a system where these numbers could fluctuate, allowing flips of side chains from left to right or vice versa. They found that in the latter case spontaneous curvature occurs, whereas in the former case, it is absent. If one considers a frozen-in uneven distribution of side chains to both sides of the backbone, then spiral conformations occur,<sup>27</sup> thus accounting for the corresponding experimental observations.<sup>11</sup> However, the strictly 2D case (where in the “top view” of the polymer adsorbed to the surface chain “crossings” are strictly forbidden) may differ somewhat from the limit of very strong adsorption (where in the “top view” chain “crossing” may still occur, requiring only at the crossing points monomers that still are nonadsorbed to respect the excluded volume interaction). In the present work, we shall investigate the latter case.

The present work uses the same model that was studied in our previous work,<sup>24</sup> disregarding now the vicinity of the adsorption transition but rather presenting a systematic analysis of the structure of adsorbed molecular bottle brushes by varying  $N_b$  systematically over a wide range for side chain lengths  $N = 6, 12, 18$ , and 24, which nicely match the range that is experimentally accessible.<sup>28–30</sup> Our aim is to clarify the structure of both “weakly adsorbed” and “strongly adsorbed” molecular brushes (what we mean by “weakly” and “strongly” adsorbed has been defined above), from the monomeric scale up to the global conformation. We shall also compare our results for the “stiffness” of the adsorbed bottle brushes (as characterized by backbone bond orientational correlations, various estimates for the persistence length, etc.) to corresponding results for nonadsorbed bottle brushes in 3D space.<sup>30,31</sup>

In Section 2, we recapitulate the model that is used, whereas Section 3 presents our numerical results. Our conclusions will be summarized in Section 4, where a comparison to the 3D case is presented, and also an outlook on pertinent experimental work and its analysis is given.

## 2. MODEL AND SIMULATION METHODS

Following Hsu et al.,<sup>24,30,31</sup> we use the bond fluctuation model on the simple cubic lattice,<sup>32–34</sup> where each (effective) monomer blocks all eight sites of an elementary cube of the lattice for further occupation, and the lattice spacing is the unit of length. The adsorbing surface is the lattice plane  $z = 0$ , and one chain end of the backbone is grafted onto the surface at a fixed position. The bond vectors connecting two adjacent monomers (which can occur only with  $z$  coordinates  $z \geq 0$ ) are chosen from the set  $\{(2,0,0); (2,1,0); (2,1,1); (2,2,1); (3,0,0); \text{ and } (3,1,0)\}$  including also all possible rotations, reflections, and reversions of these bond vectors. We use the same set of bond vectors, irrespective of whether the backbone or a side chain is considered and do not allow for any other monomer–monomer interaction apart from excluded volume: thus, any effects resulting from different chemical structure of backbone polymer and side chains are ignored, and because of the lack of any attractive forces between monomers, we clearly consider only the good solvent regime. Apart from the two end monomers of the backbone, one side chain is grafted on each backbone monomer. Therefore, the total number of monomers per chains is  $N_{\text{tot}} = N_b + N(N_b - 2)$ . Whereas in the bulk we succeeded to equilibrate chains as large as  $N_b = 1027, N = 24$  ( $N_{\text{tot}} = 25\,627$ ), in the present work, the largest bottle brush simulated is only  $N_b = 643, N = 18$  ( $N_{\text{tot}} = 12\,181$ ) because it is significantly more difficult to equilibrate adsorbed chains rather than free chains. Adsorption is controlled by an energy  $\varepsilon$  that is won if a monomer has (four) sites in the plane  $z = 0$ . (The remaining four sites of the cube then are necessarily in the plane  $z = 1$ .) No energy occurs for monomers that do not have sites in the plane  $z = 0$ , so unlike other studies of polymer adsorption (e.g., ref 35), our adsorption potential is an extremely short-ranged “contact potential”.

Details of the preparation of the initial configuration and the subsequent approach toward equilibrium can be found in our previous work.<sup>24</sup> Here we focus on two choices of the parameter  $\varepsilon$  that we varied to control the adsorption of the molecular brush, namely,  $\varepsilon = 1.25$  (weak adsorption) and 1.5 (strong adsorption), respectively. We choose units such that absolute temperature  $T = 1$  and Boltzmann’s constant  $k_B = 1$ , so a Monte Carlo move that would take one monomer off the plane  $z = 0$  is subject to the standard acceptance probability<sup>36</sup>  $P_{\text{acc}} = \min\{1, \exp(-\varepsilon)\}$ . Figure 1 explains the motivation for this particular choice of adsorption energies, showing the mean distance  $\langle z \rangle_b$  of backbone monomers as a function of  $\varepsilon$ . The almost constant behavior for  $\varepsilon \leq 0.9$  indicates that the molecular brushes are not adsorbed (only due to the grafted end a part of the macromolecule is close to the surface) but repelled from it through the entropic excluded volume interaction due to the wall. The adsorption transition, which occurs near  $\varepsilon_c = 1.00 \pm 0.02$  (within the accuracy of this estimate, no dependence on the length  $N$  of the side chains could be identified<sup>24</sup>), is rounded for any finite length of the backbone  $N_b$  and would become sharp only in the limit  $N_b \rightarrow \infty$ , as is well-known (e.g., refs 35, 37, and 38). Consequently, we see near  $\varepsilon_c = 1.0$  a rounded onset of the decrease in  $\langle z \rangle_b$ , which becomes sharper with increasing  $N_b$ . Interestingly, this decrease then

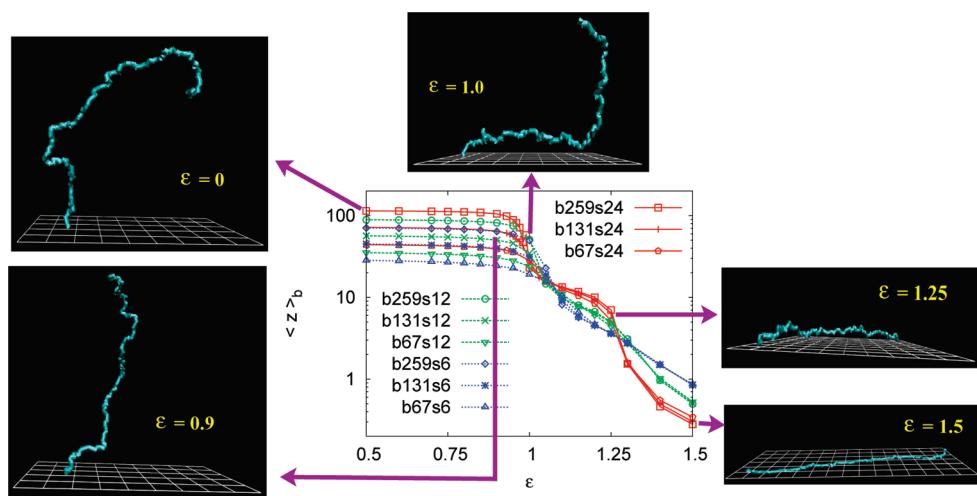


**Figure 1.** Average position  $\langle z \rangle_b$  of backbone monomers plotted versus adsorption energy  $\varepsilon$  for several choices of backbone chain length  $N_b$  and side chain length  $N$  (denoted as  $bN_b s N$  in the Figure). For the case  $N_b = 131$ ,  $N = 24$  and five choices of  $\varepsilon$ , typical snapshot pictures of the backbone chain are shown, as indicated. Note that for each effective monomer, only the  $z$  coordinate of the four lower sites of the cube is counted. Note the logarithmic scale of the ordinate in the Figure.

becomes flatter again for distances in the range  $5 \leq \langle z \rangle_b \leq 10$ , for adsorption energies in the range  $1.1 \leq \varepsilon \leq 1.25$ . These still rather large values of  $\langle z \rangle_b$  indicate that actually most of the backbone monomers are not yet adsorbed to the surface, whereas the analysis of the global configuration of the macromolecule (data on the mean-square gyration radius resolved in components perpendicular ( $z$ ) and parallel ( $\parallel$ ) to the surface,  $\langle R_{gz}^2 \rangle$  and  $\langle R_{g\parallel}^2 \rangle$ , see ref 24) implies that the bottle brush polymer already is adsorbed to the wall. The snapshot picture of the backbone for  $\varepsilon = 1.25$  (Figure 1) nicely illustrates this conclusion. For  $\varepsilon > 1.25$ , a second rather steep decrease in  $\langle z \rangle_b$  with  $\varepsilon$  occurs, and the values  $\langle z \rangle_b < 1.0$  for  $\varepsilon = 1.5$  indicate that now most of the backbone monomers are already attached to the attractive wall. This conclusion is again corroborated by the snapshot in Figure 1 and confirmed by a quantitative analysis of the fraction of surface contacts of the backbone monomers. (See Figure 3c of ref 24). An examination of snapshot pictures of the whole molecular cylindrical brush (Figure 2) also clearly suggests that for  $\varepsilon = 1.25$  the macromolecule still is a 3D object, despite its surface attachment, whereas for larger values of  $\varepsilon$  a significant flattening occurs. Linear dimensions of the side chains in the  $z$  direction are of the same order as in parallel direction for  $\varepsilon = 1.25$  but become progressively smaller as  $\varepsilon$  increases. Ultimately (for still larger values of  $\varepsilon$  than investigated by us), the configuration of the adsorbed bottle brush becomes strictly 2D. We have not tried to study this limit, however, because of severe equilibration problems. Note that our simulation technique is a dynamical Monte Carlo method, attempting both local moves, where a monomer is displaced by only one lattice unit (the so-called “L6” move<sup>24,30,31,39</sup>), as well as by a larger distance (the “L26” move<sup>39</sup>), which ensures faster equilibration because it allows for bond crossings and nonlocal “pivot moves”.<sup>24,36</sup> We consider both pivot moves where at a randomly chosen backbone monomer part of the backbone (plus attached side chains) are moved to a new position and pivot moves that create a new configuration for a side chain (or part thereof). Note that the presence of pivot moves and L26 moves are particularly important for the case of strongly adsorbed (almost 2D) chains to maintain ergodicity, avoiding the frozen states that one observed otherwise.<sup>40</sup> In  $d = 3$

dimensions, these pivot moves are just derived from the 48 symmetry operations of the simple cubic lattice: rotations by 90 or 180° around any of the cubic axes, reflections, inversions, or no change at all. To avoid an inappropriate bias, both the pivot points and the type of move need to be chosen at random. However, for adsorbed chains, the acceptance rate for most types of these moves becomes extremely small. In the case of strong adsorption, rotations by 90° around the  $z$ -axis leave the number of monomers bound to the surface invariant as well as 180° rotations around the  $x$  or  $y$  axis; nevertheless, the acceptance rate of these moves is extremely small because of excluded volume constraints. For  $\varepsilon > 1.5$ , a very extensive analysis of autocorrelation functions is necessary to ensure that the runs are actually long enough that full thermal equilibrium is reached. Of course, these equilibration problems have a counterpart in experimental studies, where irreversible adsorption leading to essentially frozen structures may be a problem as well.

### 3. SIMULATION RESULTS FOR THE CONFORMATIONAL PROPERTIES OF ADSORBED BOTTLE BRUSH POLYMERS

Figures 3–5 show our “raw data” for the linear dimensions of the chain backbone, which demonstrates that the perpendicular linear dimensions with increasing backbone chain length  $N_b$  converge to a plateau value that increases with side-chain length  $N$  for the weak adsorption case  $\varepsilon = 1.25$ , whereas the plateau value decreases with  $N$  for the strong adsorption case (Figure 3). The obvious interpretation is that in the weakly adsorbed case the side chains still have a (almost) 3D conformation, and hence with increasing  $N$  it is favorable that the grafting sites for the side chains are more remote from the surface. A similar “shielding” of the backbone by the side chains was already found by Saariaho et al.<sup>41</sup> for bottle brush polymers confined in a thin film geometry between purely repulsive walls. In contrast, for the most strongly adsorbed case,  $\varepsilon = 1.5$ , it is preferable to have the side chains in a sense “pull” the backbone chain down to the surface. In this way, one can understand that the trend of  $\langle R_{gb,\perp}^2 \rangle$  with  $N$  is opposite in both cases.

When we study the parallel components (Figure 4), the trend in both cases is qualitatively similar: for not so large  $N_b$ , there is a significant increase in  $\langle R_{gb,\parallel}^2 \rangle / (2l_b N_b^{2\nu_2})$  with  $N_b$ , indicating that the structure of these bottle brushes is rodlike. Of course, for simple linear polymers ( $N = 0$ ), such a rodlike regime is absent; also, when the side chains are rather short (e.g.,  $N = 6$  and 12) the rodlike regime stops already at relatively small  $N_b$ . The fact that

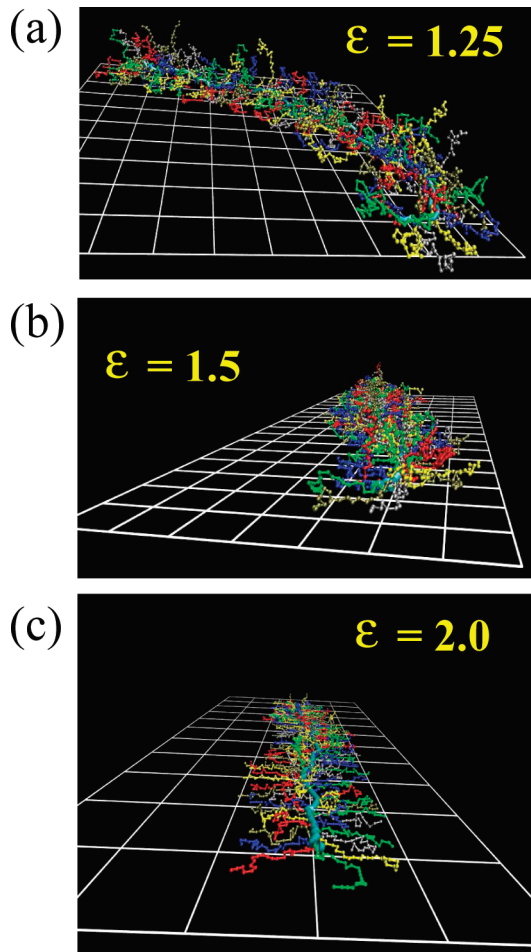


**Figure 2.** Snapshot pictures of adsorbed bottle brushes for the case of  $N_b = 131$ ,  $N = 24$ , and three choices of  $\varepsilon$ :  $\varepsilon =$  (a) 1.25, (b) 1.50, and (c) 2.0.

plateaus are reached after a factor  $N_b^{2\nu_2}$  with  $\nu_2 = 3/4$  has been divided out indicates that in both cases a crossover of the backbone conformations to a self-avoiding walk-type behavior in  $d = 2$  dimensions has occurred. The same conclusion emerges from the mean-square end-to-end distance (Figure 5). Defining an effective persistence length  $l_{p,R}$  via<sup>31</sup>

$$\langle R_{eb,\parallel}^2 \rangle = 2l_b l_{p,R} N_b^{2\nu_2} \quad (1)$$

we find that  $l_{p,R}$  is only of the order of a few bond lengths  $l_b$  throughout: thus one should not be misled from the picture emerging from single snapshots to misinterpret our data by concluding that a very strong backbone stiffening occurs.

Another basic quantity to consider is the number of monomer–surface contacts, distinguishing again between the backbone (Figure 6) and the side chains (Figure 7). Consistent with our discussion of  $\langle R_{gb,\perp}^2 \rangle$ , the trends for weak ( $\varepsilon = 1.25$ ) and strong ( $\varepsilon = 1.5$ ) adsorption are opposite in Figure 6: with increasing  $N$  the ratio  $\langle N_s \rangle_b / N_b$  decreases for  $\varepsilon = 1.25$  but increases for  $\varepsilon = 1.5$ . In contrast, for the side-chain monomers,  $\langle N_s \rangle_c / [N(N_b - 2)]$  decreases with  $N$  in both cases; however, for  $\varepsilon = 1.25$ , this ratio clearly converges to a value that is small in comparison with unity as  $N \rightarrow \infty$ , whereas for  $\varepsilon = 1.5$ , it converges to a value near 0.3. Therefore, even in the more strongly adsorbed case ( $\varepsilon = 1.5$ ) our model system is very different from a strictly 2D system, where  $\langle N_s \rangle_c / [N(N_b - 2)] = 1$ . We have also investigated the counterpart of Figure 6 for the free ends of the side chain (not shown here), but we have found that the free ends do not behave much differently from the inner monomers of the side chains. We also remark that the convergence of all of these data to their asymptotic values (reached strictly only for  $N_b \rightarrow \infty$ ) is very rapid for the side chains ( $N = 6, 12$ ) but becomes progressively slower with increasing  $N$ . For  $N = 24$ , we could not study large enough  $N_b$  to quote a meaningful estimate for the plateau values at all.

Finally, as a further geometric characteristic, we discuss the average height  $\langle z \rangle$  of monomers above the surface, distinguishing again between backbone monomers  $\langle z \rangle_b$  (Figure 8) and side-chain monomers  $\langle z \rangle_c$  (Figure 9). Again, for  $\langle z \rangle_b$ , the trend with  $N$  at  $\varepsilon = 1.25$  and 1.5 is opposite. For  $\varepsilon = 1.25$ , we find that  $\langle z \rangle_b$  converges with increasing  $N_b$  to plateau values that increase with  $N$ , indicative for more or less 3D configurations of the side chains. For  $\varepsilon = 1.5$ , however,  $\langle z \rangle_b < 1$  for all of our bottle brushes, and  $\langle z \rangle_b$  decreases with increasing  $N$ , indicative of a convergence

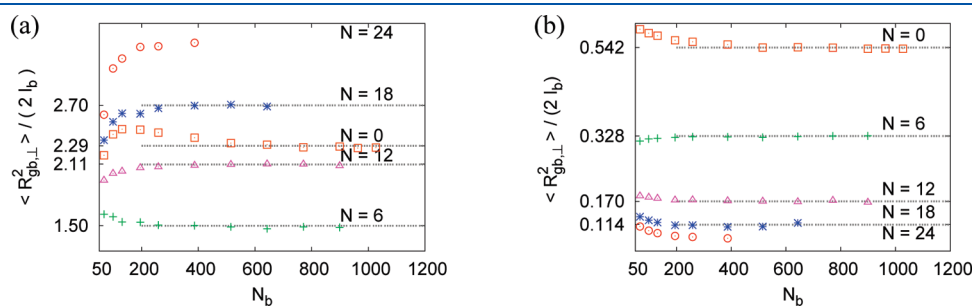


**Figure 3.** Mean-square gyration radius components  $\langle R_{gb,\perp}^2 \rangle$  of the backbone in the  $z$  direction perpendicular to the surface plotted versus backbone chain length  $N_b$  for several choices of side chain length  $N$ , as indicated. (Also, the case of a simple linear polymer without side chains is included and denoted as  $N = 0$ .) The data are normalized by  $2l_b$ , where  $l_b$  ( $\sim 2.7$  lattice spacings) is the average bond length. Case (a) refers to  $\varepsilon = 1.25$ , and case (b) refers to  $\varepsilon = 1.5$ . Note the difference in ordinate scales in both parts of the Figure. The horizontal plateaus (entries at the ordinate) indicate tentative estimates for the limiting behavior for  $N_b \rightarrow \infty$ , implying that the thickness of the resulting “pancake” configuration of the adsorbed polymer increases with  $N$  for  $\varepsilon = 1.25$ , whereas for  $\varepsilon = 1.5$ , an essentially 2D configuration results.

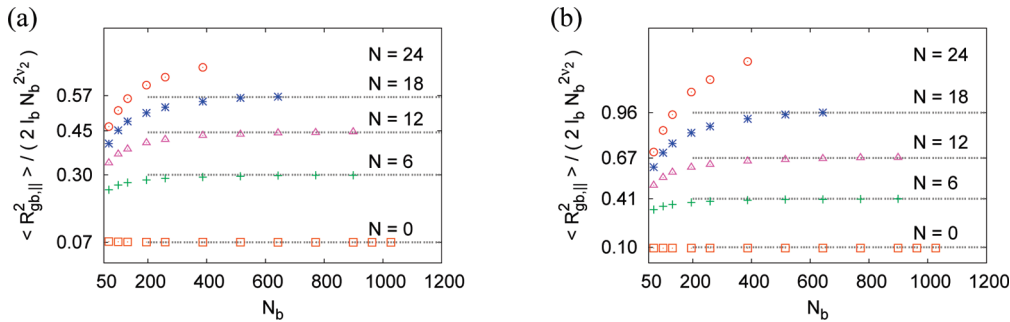


**Figure 4.** Mean-square gyration radius components  $\langle R_{gb,||}^2 \rangle$  of the backbone in the  $x,y$  directions parallel to the surface plotted versus backbone chain length  $N_b$  for several choices of side chain length  $N$  as indicated. The data are normalized by a factor  $2l_b N_b^{2\nu_2}$  with  $\nu_2 = 3/4$ , so that the horizontal plateaus (entries at the ordinate) reached show that the backbone behaves like a 2D self-avoiding walk. Case (a) refers to  $\epsilon = 1.25$  and case (b) to  $\epsilon = 1.5$ . Note the difference in ordinate scales in both parts of the Figure.

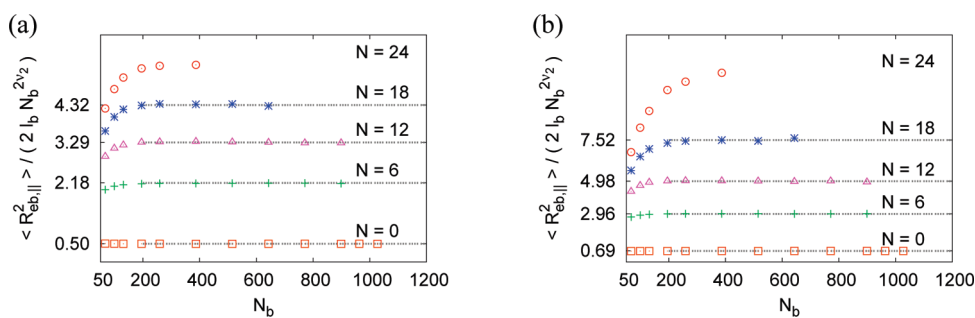


**Figure 5.** Same as Figure 4, but for the mean-square end-to-end distance components  $\langle R_{eb,||}^2 \rangle / (2l_b N_b^{2\nu_2})$ . Estimates for the asymptotic values for  $N_b \rightarrow \infty$  are shown by dotted horizontal lines and quoted at the ordinate axis.

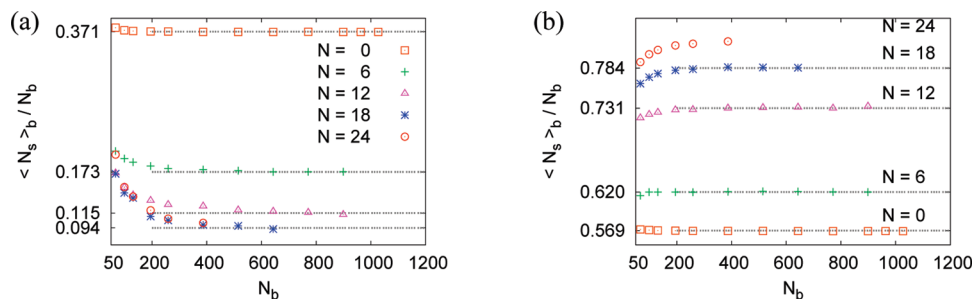


**Figure 6.** Fraction of monomer–surface contacts for the monomers on the backbone,  $\langle N_s \rangle_b / N_b$ , plotted versus backbone chain length  $N_b$ . Various choices of side chain length are included, as indicated. Case (a) refers to  $\epsilon = 1.25$  and case (b) refers to  $\epsilon = 1.5$ , respectively. Estimates for the asymptotic values for  $N_b \rightarrow \infty$  are shown by dotted horizontal lines and quoted at the ordinate axis.

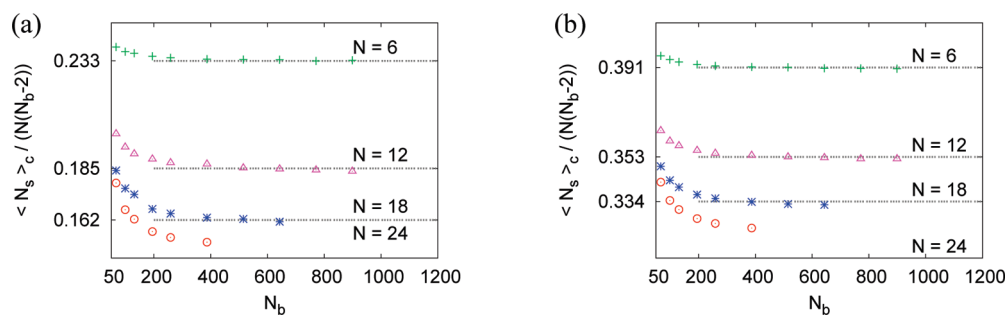


**Figure 7.** Same as Figure 6 but for side-chain monomers,  $\langle N_s \rangle_c / (N(N_b - 2))$ .

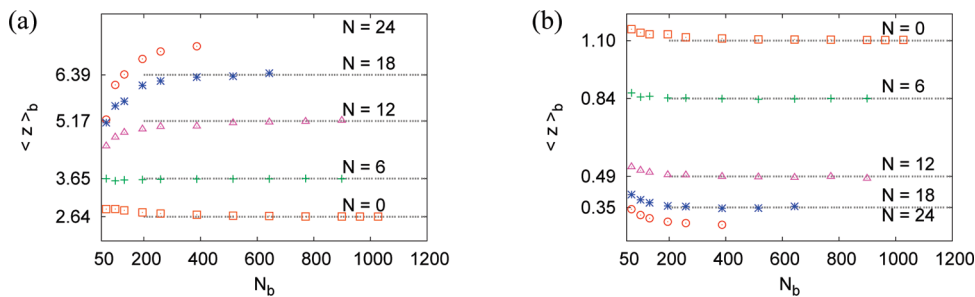


**Figure 8.** Average height  $\langle z \rangle_b$  of backbone monomers plotted versus backbone chain length  $N_b$  for  $\varepsilon =$  (a) 1.25 and (b) 1.5. Several choices of side-chain length are included, as indicated. Estimates for the asymptotic values for  $N_b \rightarrow \infty$  are shown by dotted horizontal lines and quoted at the ordinate axis.

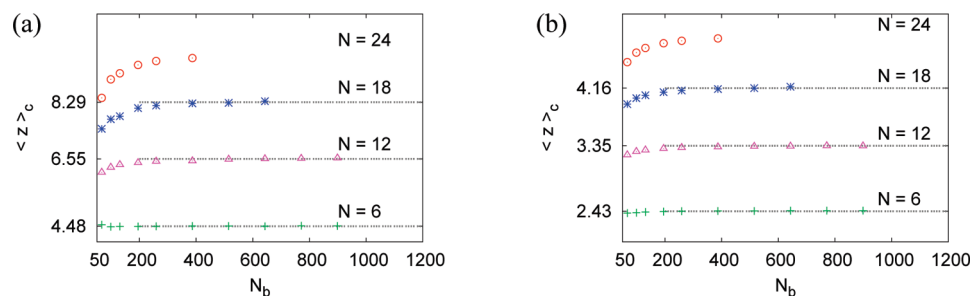


**Figure 9.** Same as Figure 8 but for side-chain monomers.

against a strictly 2D behavior. For the side chains, we find a strong increase in  $\langle z \rangle_c$  with  $N$  for  $\varepsilon = 1.25$  and a weaker increase for  $\varepsilon = 1.5$  (Figure 9). Once more, we have also computed  $\langle z \rangle_{c,e}$  taking only the free ends of the side chains into account (not shown), but we have again found that there is not much difference to the average obtained from all of the side chain monomers.

Given the fact that for  $\varepsilon = 1.25$  the side chains take more or less 3D configurations and “pull” the backbone away from the surface, why does the bottle brush then adsorb at all? The answer is that what matters in an adsorption transition is the “crossover scaling variable”  $\zeta = (\varepsilon/\varepsilon_c - 1)N_{\text{tot}}^\phi$ , where  $\varepsilon_c (\sim 1.0)$  is the critical value of the adsorption energy and  $\phi$  is the “crossover exponent”<sup>35,37,38</sup> ( $0.5 \leq \phi \leq 0.59$ ): Adsorption is taking place for  $\zeta \gg 1$ . Because there is no distinction in our adsorption potential between monomers of the backbone or monomers of the side chains, a bottle brush polymer for which  $N_b$  is very large and  $N \gg 1$  as well, for a conformation where the backbone is essentially oriented parallel to the surface and occurs at a vertical distance of the order of  $\langle R_{gc}^2 \rangle^{1/2}$  of a side chain above the surface, there will still occur enough contacts between monomers of side chains and the wall such that the number of surface contacts  $\langle N_s \rangle_c$  is very large in comparison with unity because of the large number of side chains. When we consider only those side chains that have surface contacts and the backbone connecting their grafting sites, the picture is not essentially different from the classical description of a weakly adsorbed linear chain in terms of loops and trains (and tails). The different chemical architecture of the nonadsorbed part of the bottle brush polymer then does not matter, as far as the location ( $\varepsilon_c$ ) of the adsorption transition is concerned, and thus we can give a better physical interpretation to one of the main findings of our previous work.<sup>24</sup>

From Figure 7, it is evident that even for  $\varepsilon = 1.5$  and side-chain lengths  $N \geq 12$ , a fraction of only  $\sim 1/3$  of the side-chain

monomers is adsorbed (whereas the fraction of backbone monomers that is adsorbed is much larger, Figure 6). Therefore, most of the side chains start out from wall-attached monomers, even though these side chains are rather incompletely adsorbed. In view of this fact, it is interesting to consider the question of what the typical shape of such a partially adsorbed “mushroom” formed by a single-side chain is. Figure 10 plots the ratio of the mean square gyration radii  $\langle R_{gc,\perp}^2 \rangle / \langle R_{gc,\parallel}^2 \rangle$  in the  $z$  direction perpendicular to the surface ( $\langle R_{gc,\perp}^2 \rangle$ ) and the  $x-y$ -directions parallel to the surface ( $\langle R_{gc,\parallel}^2 \rangle$ ) as a function of backbone chain length  $N_b$  for both  $\varepsilon = 1.25$  and 1.5. There are two surprising features: (i) Apart from the case  $N = 6$ , the convergence of this ratio to a limiting value with increasing  $N_b$  is very slow. (ii) The dependence on  $\varepsilon$  is rather weak; for  $\varepsilon = 1.25$ , typical values of this ratio are in the range 0.34 to 0.38 and for  $\varepsilon = 1.5$  in the range 0.23 to 0.31. As a consequence, we must again emphasize that the side-chain conformations are far from quasi-2D in both cases; then, this ratio would be much smaller. When we analyze the mean square end-to-end distance of the side chains, the picture is very similar to Figure 10; therefore, it is not shown. These findings imply that the transition of the backbone chain from a weakly to a strongly adsorbed state that takes place between  $\varepsilon = 1.25$  and 1.5 does not affect the side-chain conformations very much.

This conclusion is corroborated by the study of cross-sectional monomer density profiles (Figure 11). Here we extend the idea of Hsu et al.<sup>42</sup> to introduce a local coordinate system (for each conformation of the bottle brush) where one coordinate (which we denote as the  $x$  axis now) follows the (coarse-grained) projection of the chain backbone onto the  $x-y$  plane. Whereas in the bulk<sup>42</sup> one could then record a radial monomer density profile in the plane perpendicular to the backbone, one now must consider that the direction (the  $y$  axis) perpendicular to the (projected) backbone, but on the  $x-y$  surface plane and the

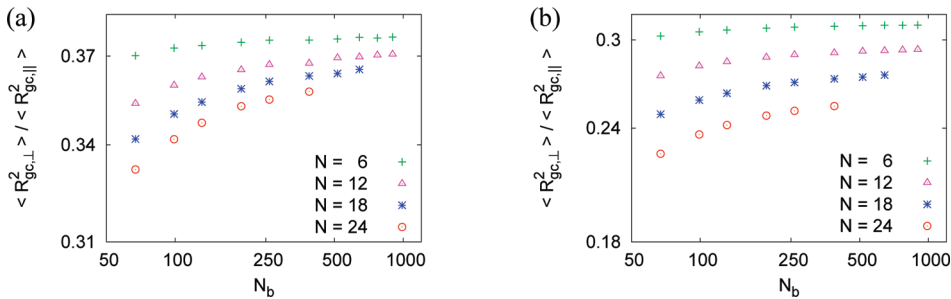


**Figure 10.** Ratio between the mean square gyration radius component perpendicular and parallel to the surface,  $\langle R_{g,\perp}^2 \rangle / \langle R_{g,\parallel}^2 \rangle$  plotted versus backbone chain length  $N_b$  for the bottle brush side chains on log–log scales: Side chain lengths  $N$  are indicated. Case (a) refers to  $\epsilon = 1.25$ , and case (b) refers to  $\epsilon = 1.5$ .

direction perpendicular to the surface plane (the  $z$  axis) is not equivalent. Figure 11 shows typical examples for the resulting monomer density distributions  $\rho(y,z)$  where  $2 \int_0^\infty \int_0^\infty dz dy \rho(y,z) = 1$ . One can see that with increasing  $\epsilon$  the density in the plane  $z = 0$  gradually increases, and the density in the layers with  $z > 0$  slowly decreases, but even for  $\epsilon = 2.0$ , we are far from a strictly 2D state.

As a final point, we discuss the inadequacy of the Kratky–Porod model<sup>19</sup> to describe conformations of adsorbed bottle brush polymers. First of all, we recall the concept of extracting a persistence length  $l_p$  from the asymptotic decay of the bond vector autocorrelation function

$$\langle \cos \theta(s) \rangle = \frac{1}{N_b - 1 - s} \sum_{i=1}^{N_b - 1 - s} \langle \vec{a}_i \cdot \vec{a}_{i+s} \rangle / \langle \vec{a}_i^2 \rangle, \\ \langle \vec{a}_i^2 \rangle \equiv l_b^2 \quad (2)$$

In eq 2,  $\vec{a}_i$  is the bond vector connecting monomer  $i$  to monomer  $i + 1$ , and we have denoted by  $N_b$  the total number of monomers in the backbone, so  $N_b - 1$  bond vectors can be defined. The “chemical distance” between monomers (that are consecutively labeled) is denoted by  $s$ . Assuming Gaussian chain statistics, one defines<sup>43</sup>  $l_p$  from the exponential decay of  $\langle \cos \theta(s) \rangle$  with the contour length  $sl_b$  along the chain

$$\langle \cos \theta(s) \rangle \propto \exp(-sl_b/l_p), \quad 1 \ll s \ll N_b \quad (3)$$

Unfortunately, eq 2 fails in the presence of excluded volume interaction (see refs 20, 21, and 31 and references therein), and one rather has

$$\langle \cos \theta(s) \rangle \propto s^{-\beta}, \quad \beta = 2(1 - \nu) = 1/2, \quad 1 \ll s \ll N_b \quad (4)$$

where we have taken into account that the backbone conformation is quasi-2D in our case, and hence  $\nu = \nu_2 = 3/4$  in eq 4 to be used. Figure 12 shows a plot of  $\langle \cos \theta(s) \rangle$  versus  $s$  for our model. Clearly, eq 3 is inadequate to describe the data; however, still much larger values of  $N_b$  would be desirable to see eq 4 clearly.

As has already been noted for nonadsorbed free bottle brush polymers in 3D space, there occurs a very rapid initial decay for small  $s$  ( $s = 1, 2$ , and 3). This rapid initial decrease in  $\langle \cos \theta(s) \rangle$  from unity (for  $s = 0$ ) to a value near 0.5 reflects the fact that on a very small scale the backbone remains flexible even if on a coarse-grained scale the cylindrical brush is rather stiff (as it must be when one considers the snapshots Figures 1 and 2). Then, one encounters a regime where a fit to eq 3 is possible, but both the range over which this regime extends and the decay constant (the persistence length  $l_p$ ) that one can extract from a fit to eq 3

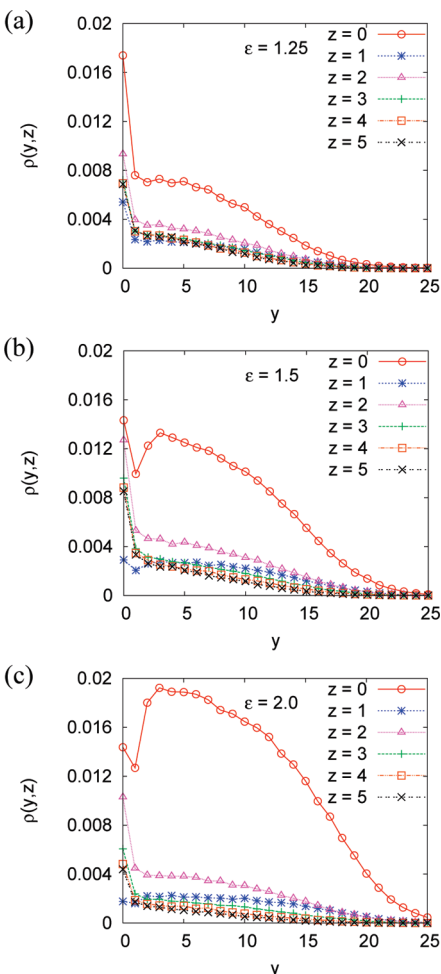


**Figure 11.** Cross-sectional monomer density distribution  $\rho(y,z)$  in the plane perpendicular to the (coarse-grained<sup>42</sup>) backbone of the bottle brush, projected onto the  $x$ – $y$  plane, plotted as function of  $y$  for  $N_b = 259$ ,  $N = 12$ , and six choices of  $z$  as indicated, for  $\epsilon =$  (a) 1.25, (b) 1.5, and (c) 2.0.  $\rho(y,z)$  is normalized such that  $2 \int_0^\infty \int_0^\infty dy dz \rho(y,z) = 1$ .

distinctly depend on  $N_b$ , and hence the fitted value of  $l_p$  is not a reliable measure of the local “intrinsic” stiffness of the chain. For the case of free bottle brush polymers in 3D solutions, this problem was already noted in our previous work,<sup>30,31</sup> and here we show that the same difficulty applies to adsorbed bottle brushes as well. For large  $s$ , comparable to  $N_b$ , distinct downward

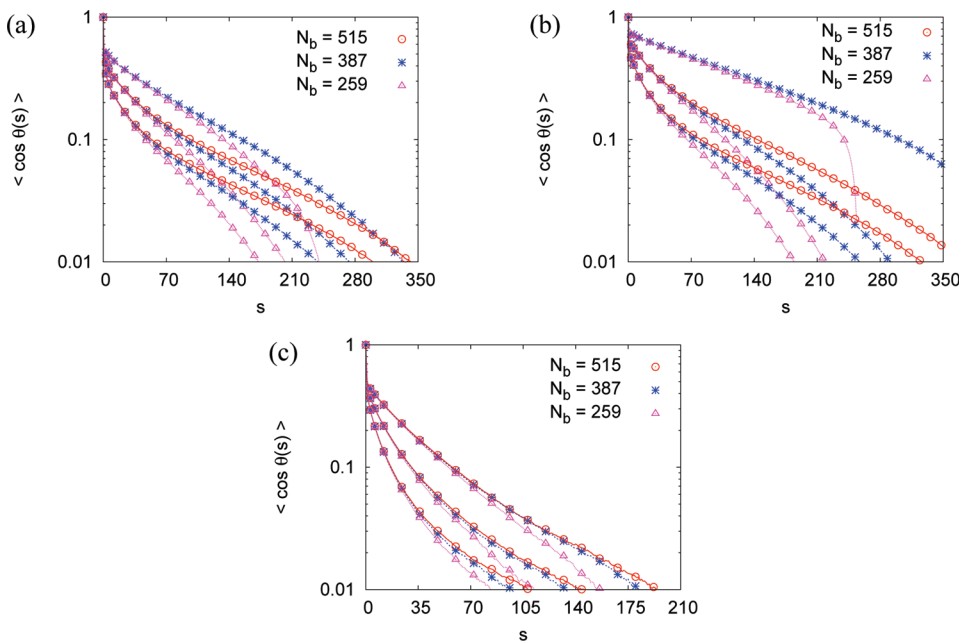


**Figure 12.** Bond vector correlation function  $\langle \cos \theta(s) \rangle$  of the backbone plotted against the “chemical distance”  $s$  along the backbone for  $\varepsilon$  = (a) 1.25 and (b) 1.5. Three sets of data for side chain lengths  $N = 24, 12$ , and 6 from up to down are shown for backbone lengths  $N_b = 259, 387$ , and 515. For the sake of comparison, case (c) shows corresponding data for a nonadsorbed free bottle brush polymers in 3D solutions.

curvature on the semilog plot of  $\langle \cos \theta(s) \rangle$  versus  $s$  indicates that bond orientations get uncorrelated when  $s$  approaches  $N_b$ , as expected.

When one examines the data for  $N = 6$  and 12 more closely, one recognizes that the slope  $|d(\ln\langle \cos \theta(s) \rangle)/ds|$  first steadily decreases with  $s$  until it reaches a minimum (near about  $S_{\min} \approx N_b/3$ ) before the final decrease in slope (reflecting the loss of orientational correlation due to the finite backbone chain length) sets in. This initial decrease in the slopes of course is a consequence of the fact that the long-range correlations due to excluded volume interactions require that for  $N_b \rightarrow \infty$  the power law, eq 4, must hold. Figure 13 shows that indeed the decrease in the slope  $|d(\ln\langle \cos \theta(s) \rangle)/ds|$  with  $s$  in the regime  $10 < s < 100$  can be attributed to the power laws (eq 4). For  $s \geq 100$ , there occurs for the bottle brushes a strong decrease in  $\langle \cos \theta(s) \rangle$  because of the fact that  $N_b$  is not large enough, but the data for  $N \equiv 0$  and the corresponding self-avoiding walks data show the power law more clearly.

An alternative way of estimating a persistence length for ideal chains would be to attempt fitting the data for the end-to-end distance of the backbone to the formula resulting for the Kratky–Porod model<sup>19</sup> ( $L = N_b l_b$  is the contour length of the backbone)

$$\langle R_{eb,||}^2 \rangle = 2l_p L \left\{ 1 - \frac{l_p}{L} [1 - \exp(-L/l_p)] \right\} \quad (5)$$

Same as for 3D bottle brush polymers in bulk solution, we will contrast this procedure to a physically more correct description, where we search for a scaling behavior that describes the crossover from the rigid rodlike behavior for small  $N_b$ , to the self-avoiding walk-like behavior pertaining at  $N_b \rightarrow \infty$ <sup>19</sup> because eq 5 rather describes a crossover from rigid rods (for  $L < l_p$  to Gaussian chains ( $\langle R_{eb,||}^2 \rangle = 2l_p L \equiv 2l_p N_b$ ), which obviously cannot be a correct description of our data (Figure 4). To derive the

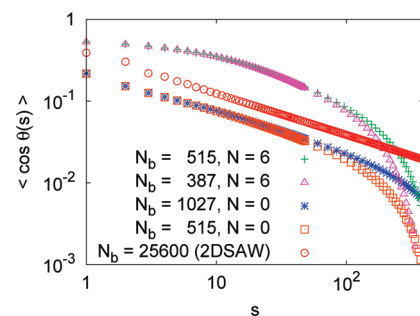


**Figure 13.** Log–log plot of  $\langle \cos \theta(s) \rangle$  versus  $s$  for the case  $N = 0$  (simple adsorbed chain at  $\varepsilon = 1.5$ ) for  $N_b = 515$  and 1027, respectively, and for  $N = 6$ ,  $N_b = 387$  and 515. The case of a simple 2D self-avoiding walk on the square lattice (where for the chosen scale of  $s$  finite chain length effects are negligible because  $N_b = 25\,600$  was chosen<sup>21</sup>) is shown for comparison.

correct crossover scaling for bottle brush polymers, it was suggested<sup>5,20</sup> to rescale the bottle brush polymer as a self-avoiding walk of blobs, where the blob-diameter was chosen to be just the cross-sectional diameter of the bottle brush. It is not completely straightforward to choose the same definition for adsorbed bottle brush polymers, however, because for adsorbed bottle brushes the cross-sectional (coarse-grained) density profile lacks rotational symmetry, of course (cf. Figure 11). To avoid this problem, we take the blob radius simply equal to the end-to-end distance of the side chains in the parallel directions ( $\langle R_{eb,||}^2 \rangle^{1/2}$ ), so

$$\langle R_{eb,||}(s_{blob}) \rangle = 4 \langle R_{ec,||}^2 \rangle \quad (6)$$

where  $\langle R_{eb,||}^2(s) \rangle$  is the parallel component of the mean square end-to-end distance of a subchain of  $s$  consecutive monomers along the backbone of the chain. From the mean square radius of

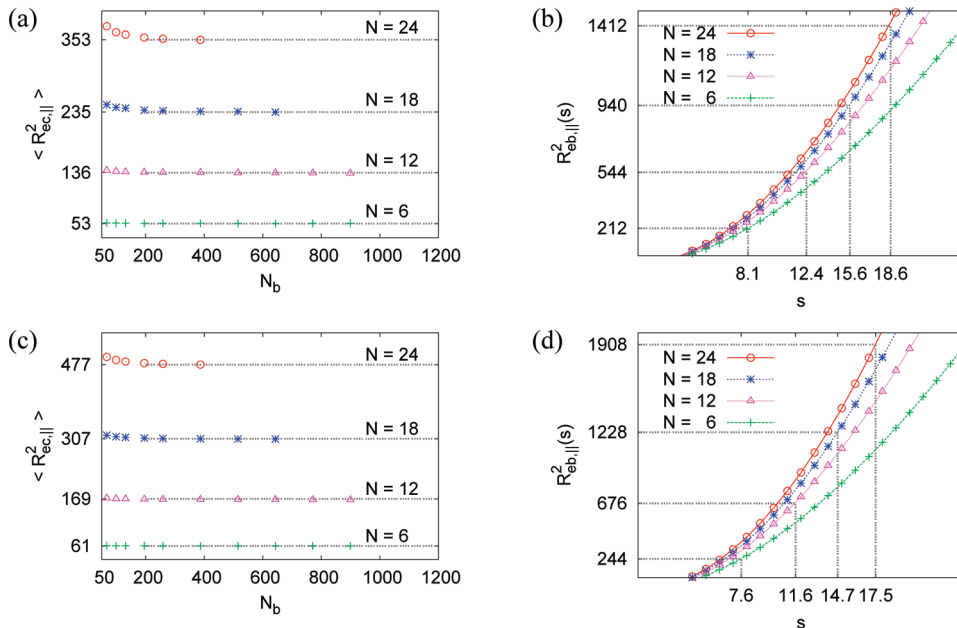


**Figure 14.** (a) Mean square end-to-end distance of the side chains in the direction parallel to the surface,  $\langle R_{ec,||}^2 \rangle$ , plotted versus backbone chain length  $N_b$ . (b) Mean square end-to-end distance of the backbone in the direction parallel to the surface,  $\langle R_{eb,||}^2(s) \rangle$ , plotted against the chemical distance  $s$ . Horizontal and vertical straight lines indicate the construction  $4\langle R_{ec,||}^2(N) \rangle = \langle R_{eb,||}^2(s_{blob}(N)) \rangle$  from which the number of monomers  $s_{blob}(N)$  is extracted.  $\varepsilon = 1.25$  in (a,b) and 1.5 in (c,d).

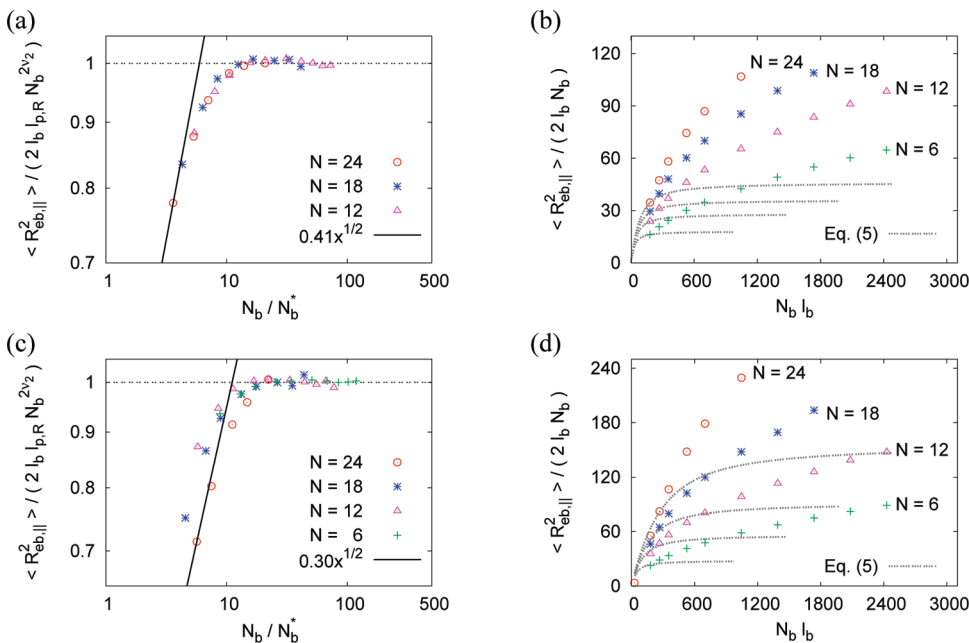


**Figure 15.** (a) Log–log plot of  $\langle R_{eb,||}^2 \rangle / (2l_p l_{p,R} N_b^{2\nu_2})$  versus  $N_b/N_b^*$  identifying  $N_b^* = s_{blob}(N)$  as estimated from Figure 14. The straight line shows the rodlike behavior. (b)  $\langle R_{eb,||}^2 \rangle / (2l_b N_b)$  versus  $N_b l_b$ . Broken curves show the rescaled Kratky–Porod model (eq 5). Here values of  $l_b$  for various side chain length  $N$  are determined by the best fit of our data.  $\varepsilon = 1.25$  in (a,b) and 1.5 in (c,d).

the side chains ( $\langle R_{ec,||}^2 \rangle$ ) we hence obtain using eq 6, the function  $s_{blob}(N)$ , as shown in Figure 14. In Figure 14a,c, we show the determination of the values  $\langle R_{ec,||}^2 \rangle(N)$ , and these values are employed in Figure 14b,d, to read off  $s_{blob}(N)$  as defined by eq 6. Figure 15 shows then a scaling plot of our data for  $\varepsilon = 1.25$  (part a) and 1.5 (part c), identifying a crossover scaling chain length  $N_b^* = s_{blob}(N)$ , to describe the crossover from the rod-like

behavior to the behavior according to 2D random walks

$$\langle R_{eb,||}^2(N_b) \rangle = 2l_p l_{p,R} N_b^{2\nu_2}, N_b/N_b^* \rightarrow \infty \quad (7)$$

$$\langle R_{eb,||}^2(N_b) \rangle = l_{b,eff}^2 N_b^2, N_b/N_b^* \leq 1 \quad (8)$$

We contrast this scaling behavior to fits employing the

**Table 1.** Estimates of  $l_{p,R}$  and  $l_{p,\text{eff}}$  for Bottle-Brush Polymers with Side Chain Lengths  $N = 6, 12, 18$ , and  $24^a$

N	6	12	18	24
$l_{p,R} (\varepsilon = 1.25)$	2.18	3.29	4.32	5.43
$l_{p,R} (\varepsilon = 1.25)$	63	106	144	185
$l_{p,R} (\varepsilon = 1.5)$	2.96	4.98	7.52	11.60
$l_{p,R} (\varepsilon = 1.5)$	111	198	291	412

<sup>a</sup> Two values of  $\varepsilon$ , 1.25 and 1.5, are chosen.

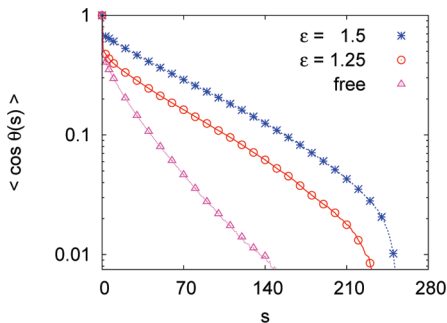


**Figure 16.** Semilog plot of the bond vector autocorrelation function  $\langle \cos \theta(s) \rangle$  of the backbone plotted against the chemical distance  $s$  for the case  $N_b = 259$ ,  $N = 18$ ,  $\varepsilon = 1.5$  and  $1.25$ , and a free chain in  $d = 3$ . This comparison shows that one cannot infer easily the orientational correlations of a free bottle brush from their adsorbed counterparts.

Porod–Kratky model in parts b and d, where it is clearly seen that this model is a valid description of our data only in the trivial rigid rod regime  $N_b l_b \rightarrow 0$ . Note that the effective bond length  $l_{b,\text{eff}} \leq l_b$  in the rigid rod regime because for small chemical distance,  $s$ , along the backbone there is only a limited rigidity. (See Figure 12.) As a consequence, also the coarse-grained contour length  $L_c$  of the bottle brush  $L_c = l_{b,\text{eff}} N_b$  in general is smaller than the nominal contour length,  $L = l_b N_b$ . Equating both expressions, eqs 7 and 8, we find another crossover chain length  $N_b^{\text{cross}}$  describing the crossover from rod-like to self-avoiding walk-like behavior for  $d = 2$  dimensions, where  $\nu = \nu_2 = 3/4$  applies

$$N_b^{\text{cross}} = (2l_{p,R} l_b / l_{b,\text{eff}}^2)^2, \quad l_{p,\text{eff}} = l_{b,\text{eff}} N_b^{\text{cross}} \quad (9)$$

where  $l_{p,\text{eff}}$  is the effective length of a rod formed from  $N_b^{\text{cross}}$  segments of length  $l_{b,\text{eff}}$  (consistent with eq 8 for  $N_b = N_b^{\text{cross}}$ ). Table 1 quotes our estimates for  $l_{p,R}$  and  $l_{p,\text{eff}}$  for  $\varepsilon = 1.25$  and  $1.5$ . The estimate for the effective length  $l_{p,\text{eff}}$  is extracted from the intersection of the two straight lines in the log–log plots such as shown in Figure 15a. However, the prediction  $l_{p,\text{eff}} \propto l_{p,R}^2$  resulting from eq 9 is not quantitatively verified.

#### 4. CONCLUSIONS

In this Article, we have analyzed the conformations of adsorbed cylindrical molecular brushes, assuming very good solvent conditions and focusing on the variation of the properties as a function of the backbone chain length  $N_b$  and side chain length  $N$ . Assuming that the chemical nature of the backbone and the side chains is identical, we considered the limiting case of extremely short-range attractive interactions between the (effective) monomers and the substrate, which for simplicity was treated as perfectly flat and structureless. Two rather distinct

cases were studied: (i) the case of “weak adsorption”, where the intrinsic local structure of the cylindrical brush still is essentially 3D, side-chain radii in the range of interest ( $6 \leq N \leq 24$  was studied here) showing a scaling  $\langle R_{\text{gc}}^2 \rangle \propto N^{2\nu}$  with  $\nu \approx 0.588$  being the exponent describing swollen coils in three dimensions, and the fraction of adsorbed monomers of the backbone is very small and (ii) the case of “strong adsorption”, the fraction of adsorbed backbone monomers being of order unity and the parallel components of the side-chain radii crossover to a scaling behavior characteristic for 2D self-avoiding walks,  $\langle R_{\text{gc},\parallel}^2 \rangle \propto N^{2\nu_2}$  with  $\nu_2 = 3/4$ . In this case, the average height  $\langle z \rangle_b$  of the backbone monomers is less than unity and decreases with increasing  $N$ , whereas for the weak adsorption case  $\langle z \rangle_b$  increases with increasing  $N$  (and then  $\langle z \rangle_c / \langle z \rangle_b$  is about 1.3 for the considered strength of adsorption energy  $\varepsilon = 1.25$  and almost independent of  $N$ , whereas in the strong adsorption case,  $\varepsilon = 1.5$ , the ratio  $\langle z \rangle_c / \langle z \rangle_b$  is in the range from 3 to 15 and increases strongly with  $N$ ). We emphasize, however, that the global conformation of the bottle brush shows a 2D self-avoiding walk-like scaling in both cases,  $\langle R_{\text{gb}}^2 \rangle \propto N_b^{2\nu_2}$  as  $N_b \rightarrow \infty$ . For small  $N_b$ , the bottle brushes behave rodlike,  $\langle R_{\text{gb}}^2 \rangle \propto N_b^2$ . The crossover from rods to (swollen) coils occurs at a backbone chain length  $N_b^{\text{cross}}(N)$ , which clearly increases strongly with  $N$ , but our side-chain lengths (which are comparable to side-chain lengths accessible in experiments) are not large enough to make statements about the asymptotic power law describing this variation for large  $N$ . Unfortunately, our results for  $l_{p,R}$  (Table 1) do not corroborate the expected relation  $l_{p,R} \propto (N_b^{\text{cross}})^{1/2}$ .

Our results do not give any evidence of a spontaneous symmetry breaking because of a “left–right asymmetry” developing in the number of adsorbed side chains along the backbone and the resulting spontaneous local curvature, showing up in strongly meandering structures. To observe this limit, we presumably need much stronger adsorption energies, leading to strictly 2D conformations of the side chains, a limit that is difficult to equilibrate (both in experiments and in simulations) and that has not been reached here.

Our results also do not confirm observations that have occasionally reported<sup>16,44</sup> a crossover from rigid rods to Gaussian-like coils ( $\langle R_{\text{eb}}^2 \rangle \propto N_b$ ) for adsorbed long semiflexible polymers. Because such a crossover occurs (if the intrinsic persistence length strongly exceeds the local thickness of the macromolecules, which is not the case for the model of bottle brushes considered here) in  $d = 3$  dimensions,<sup>5,20</sup> a possible explanation of these observations is that the macromolecules during their adsorption process have taken a structure resembling a projection of their  $d = 3$  structure on the adsorbing plane, without full equilibration in  $d = 2$ , whereas such a full equilibration was ensured in our study. We also note that in these experiments<sup>16,44</sup> a study where the stiffness was systematically varied has not been reported.

Often experiments on adsorbed semiflexible polymers (including bottle brushes<sup>14</sup>) are done with the motivation that one wishes to characterize their intrinsic stiffness, measuring their (intrinsic) “persistence length”  $l_p$ . One method that is used (e.g., ref 14) relies on the Kratky–Porod model, eq 5, describing the variation of the mean square end-to-end distance with the (coarse-grained) contour length  $L_c$  in terms of a crossover from the rod-like regime ( $L_c < l_p$ ) to Gaussian coils ( $L_c \gg l_p$ ). However, we have shown in our previous work that the Kratky–Porod description does not work for bottle brushes with flexible backbone under good solvent conditions in  $d = 3$ , and in

the present Article, we show that for adsorbed bottle brushes it fails as well. Alternatively, one sometimes tries (e.g., ref 14) to fit the bond orientational correlation function to an exponential decay over some regime, implying eq 3 to hold, to extract  $l_p$ . However, our study also implies that in general this procedure is not reliable. In particular, this orientational correlation function clearly differs for a free chain from a (weakly or strongly) adsorbed chain, as illustrated in Figure 16. In our opinion, a careful analysis of the crossover from the rod regime to the ( $d = 2$  or 3) self-avoiding walk regime is more promising.

Defining  $l_p$  by analogy to eq 9 as  $l_p = l_b N_b^{\text{cross}}$  being the value of  $N_b$  where the power law fitted to the rod-like regime in Figure 15 crosses the power law for the self-avoiding walk regime, we would get for the free bottle brush polymers in  $d = 3$  dimensions that  $l_{p,\text{eff}}/l_b \approx 22, 37, 48$ , and 59 for  $N = 6, 12, 18$ , and 24, respectively. However, whereas for the weakly adsorbed chains ( $\varepsilon = 1.25$ ) the corresponding numbers are similar,  $l_{p,\text{eff}}/l_b \approx 23, 39, 53$ , and 68, respectively, larger numbers result for the strongly adsorbed case ( $\varepsilon = 1.5$ ) (41, 73, 108, 153). As expected from Figure 16, there is no simple relation between the stiffness of an adsorbed bottle brush and its nonadsorbed counterpart because the stiffness is the result of a delicate interplay between enthalpic forces and configurational entropy, and this balance is rather different for adsorbed and free, nonadsorbed macromolecules. We hope that our study stimulates more experimental work, including an analysis of experimental data along similar lines as used for the present simulations.

## AUTHOR INFORMATION

### Corresponding Author

\*E-mail: hsu@uni-mainz.de.

## ACKNOWLEDGMENT

H.-P.H. received funding from the Deutsche Forschungsgemeinschaft (DFG), grant no. SFB 625/A3. We are grateful for extensive grants of computer time at the JUROPA under the project no. HMZ03 and SOFTCOMP computers at the Jülich Supercomputing Centre (JSC). K.B. is particularly grateful to H. E. Stanley for many illuminating discussions over a period of more than 40 years on the role of power laws and scaling in statistical physics, and W.P. is grateful for the inspirational work of H. E. S. in the area of econophysics.

## REFERENCES

- (1) Zhang, M.; Müller, A. H. E. *J. Polym. Sci., Part A: Polym. Chem.* **2005**, *43*, 3461.
- (2) Subbotin, A. V.; Semenov, A. N. *Vysokomol. Soedin., Ser. A* **2007**, *49*, 1328.
- (3) Sheiko, S. S.; Sumerlin, B. S.; Matyjaszewski, K. *Prog. Polym. Sci.* **2008**, *33*, 759.
- (4) Potemkin, I. I.; Palyulin, V. V. *Vysokomol. Soedin., Ser. A* **2009**, *51*, 123.
- (5) Hsu, H.-P.; Paul, W.; Binder, K. *Macromol. Theory Simul.* **2011**, DOI: 10.1002/mats.201000092.
- (6) Stephan, T.; Muth, S.; Schmidt, M. *Macromolecules* **2002**, *35*, 9857.
- (7) Li, C.; Gunari, N.; Fischer, K.; Janshoff, A.; Schmidt, M. *Angew. Chem., Int. Ed.* **2004**, *43*, 1101.
- (8) Proteoglycans: Structure, Biology, and Molecular Interactions; Iozzo, R. V., Ed.; Marcel Dekker: New York, 2000.
- (9) Klein, J. *Science* **2009**, *323*, 47.
- (10) Chang, R.; Kwak, Y.; Gebremichael, Y. *J. Mol. Biol.* **2009**, *391*, 648.
- (11) Khalatur, P. G.; Khokhlov, A. R.; Prokhorova, S. A.; Sheiko, S. S.; Möller, M.; Reineker, P.; Shirvanyanz, D. G.; Starovoitava, N. *Eur. Phys. J. E* **2000**, *1*, 99.
- (12) Sheiko, S. S.; Prokhorova, S. A.; Beers, K. L.; Matyjaszewski, K.; Potemkin, I. I.; Khokhlov, A. R.; Möller, M. *Macromolecules* **2001**, *34*, 8354.
- (13) Potemkin, I. I.; Khokhlov, A. R.; Prokhorova, S.; Sheiko, S. S.; Möller, M.; Beers, K. L.; Matyjaszewski, K. *Macromolecules* **2004**, *37*, 3918.
- (14) Gunari, N.; Schmidt, M.; Janshoff, A. *Macromolecules* **2006**, *39*, 2219.
- (15) Sheiko, S. S.; Sun, F. G.; Randall, A.; Shirvanyants, D.; Rubinstein, M.; Lee, H.; Matyjaszewski, K. *Nature (London)* **2006**, *440*, 191.
- (16) Gallyamov, M. O.; Tartsch, B.; Mela, P.; Potemkin, I. I.; Skeiko, S. S.; Börner, H.; Matyjaszewski, K.; Khokhlov, A. R.; Möller, M. *J. Polym. Sci., Part B: Polym. Phys.* **2007**, *45*, 2368.
- (17) Subbotin, A.; de Jong, J.; ten Brinke, G. *Eur. Phys. J. E* **2006**, *20*, 99.
- (18) (a) Potemkin, I. I. *Macromolecules* **2006**, *39*, 7178. (b) Potemkin, I. I. *Macromolecules* **2007**, *40*, 1238.
- (19) Kratky, O.; Porod, G. *J. Colloid Interface Sci.* **1949**, *4*, 35.
- (20) Hsu, H.-P.; Paul, W.; Binder, K. *EuroPhys. Lett.* **2010**, *92*, 28003.
- (21) Hsu, H.-P.; Paul, W.; Binder, K. 2011 “Breakdown of the Kratky-Porod Worm-Like Chain Model for Semiflexible Polymers in Two Dimensions”, submitted.
- (22) Feuz, L.; Leermakers, F. A. M.; Textor, M.; Borisov, O. *Langmuir* **2008**, *24*, 7232.
- (23) Elli, S.; Raffaini, G.; Ganazzoli, F.; Timoshenko, E. G.; Kuznetsov, Y. A. *Polymer* **2008**, *49*, 1716.
- (24) Hsu, H.-P.; Paul, W.; Binder, K. *J. Chem. Phys.* **2010**, *133*, 134902.
- (25) de Gennes, P. G. *Scaling Concepts in Polymer Physics*; Cornell University Press: Ithaca, NY, 1979.
- (26) de Jong, J.; Subbotin, A.; ten Brinke, G. *Macromolecules* **2005**, *38*, 6718.
- (27) Potemkin, I. I.; Khokhlov, A. R.; Reineker, P. *Eur. Phys. J. E* **2001**, *4*, 93.
- (28) Rathgeber, S.; Pakula, T.; Matyjaszewski, K.; Beers, K. L. *J. Chem. Phys.* **2005**, *122*, 124904.
- (29) Zhang, B.; Gröhn, F.; Pedersen, J. S.; Fischer, K.; Schmidt, M. *Macromolecules* **2006**, *39*, 8440.
- (30) Hsu, H.-P.; Paul, W.; Rathgeber, S.; Binder, K. *Macromolecules* **2010**, *43*, 1592.
- (31) Hsu, H.-P.; Paul, W.; Binder, K. *Macromolecules* **2010**, *43*, 3094.
- (32) Carmesin, I.; Kremer, K. *Macromolecules* **1988**, *21*, 2819.
- (33) Deutsch, H.-P.; Binder, K. *J. Chem. Phys.* **1991**, *94*, 2294.
- (34) Paul, W.; Binder, K.; Heermann, D. W.; Kremer, K. *J. Phys. II* **1991**, *1*, 37.
- (35) Descas, R.; Sommer, J.-U.; Blumen, A. *Macromol. Theory Simul.* **2008**, *17*, 429.
- (36) Monte Carlo and Molecular Dynamics Simulations in Polymer Science; Binder, K., Ed.; Oxford University Press: New York, 1995.
- (37) Eisenriegler, E.; Kremer, K.; Binder, K. *J. Chem. Phys.* **1982**, *77*, 6296.
- (38) Metzger, S.; Müller, M.; Binder, K.; Baschnagel, J. *J. Chem. Phys.* **2003**, *118*, 8489.
- (39) Wittmer, J. P.; Beckrich, P.; Meyer, H.; Cavallo, A.; Johner, A.; Baschnagel, J. *J. Phys. Rev. E* **2007**, *76*, 011803.
- (40) Lai, P.-Y. *Macromol. Theory Simul.* **1996**, *5*, 255.
- (41) Saariaho, M.; Ikkala, O.; ten Brinke, G. *J. Chem. Phys.* **1999**, *110*, 1180.
- (42) Hsu, H.-P.; Binder, K.; Paul, W. *Phys. Rev. Lett.* **2009**, *103*, 198301.
- (43) Grosberg, A. Yu.; Khokhlov, A. R. *Statistical Physics of Macromolecules*; AIP Press: New York, 2004.
- (44) Yoshinaga, N.; Yoshikawa, K.; Kidoaki, S. *J. Chem. Phys.* **2002**, *116*, 9926.